

Experimental and Theoretical Study of Fine Interfacial Waves on Thin Liquid Sheet*

Hiroyuki HASHIMOTO** and Takashi SUZUKI***

A fine interfacial wave pattern was observed on the thin liquid sheet jet in a cocurrent gas stream. The experimental observation revealed that this wave motion affected on the disintegration of the liquid sheet. To clarify the factor affecting the liquid sheet wave motion and disintegration, the fine interfacial waves were investigated experimentally. The fundamental mechanism of the fine interfacial waves was described. Then, the instability of the plane liquid sheet was also analyzed by numerically solving the Orr-Sommerfeld equation. Comparing the theoretical results with the experimental results, the hydrodynamical mechanism of interfacial wave occurrence was explained. Also, it was suggested that the interfacial wave was caused by the internal instability of the plane liquid sheet.

Key Words: Jet, Wave, Stability, Flow Visualization, Numerical Analysis, Atomization, Turbulence, Transition

1. Introduction

The behavior of a liquid jet in gaseous medium has been an interesting problem concerning spray device, jet cutting technology and so on.⁽¹⁾ In particular, the disintegration of thin liquid sheet jets in a gas flow is a very important problem concerning the improvement of the two-fluid atomizer. Recently, the authors studied the behavior of a liquid sheet in a cocurrent gas stream (in this study, a plane thin liquid sheet jet is called the liquid sheet). It was confirmed that the large-amplitude liquid sheet wave was due to the Kelvin-Helmholtz instability, and that the growth of the wave played a very important role in the disintegration of liquid sheet.^{(2),(3)} In careful photographic observation, the existence of a fine interfacial wave pattern could be confirmed on the liquid sheet in the vicinity of the nozzle exit.⁽⁴⁾ This fine wave pattern

seemed to be one of the significant factors governing the behavior of the liquid sheet. Many studies have been reported on liquid sheet disintegration. However, there are a number of unsolved problems regarding the disintegration process of a liquid sheet because of the complicated mechanisms involved. Further fundamental studies on the fine interfacial waves are needed to clarify the disintegration process in greater detail.

The final purpose of this study is to clarify the characteristics of fine interfacial waves and to obtain basic knowledge concerning disintegration in order to improve the spray devices. First, the effect of the fine interfacial waves on the disintegration of the liquid sheet in a cocurrent gas stream was examined experimentally. Then, the interfacial wave pattern of a liquid sheet in a stationary atmosphere was observed in detail. The configuration and the growth process of interfacial waves were examined experimentally. It was attempted to explain the instability of liquid sheet by the linear theory. The numerical results on the wave configuration and the wave number agreed with the experimental results. Finally, it was confirmed that the interfacial wave on a liquid sheet was mainly due to the growth of internal disturbances of the liquid sheet.

* Received 8th November, 1990. Paper No.89-1030A, 89-1031A

** Institute of Fluid Science, Tohoku University, 2-1-1 Katahira, Aoba-ku, Sendai 980, Japan

*** Department of Energy Engineering, Toyohashi University of Technology, Tenpaku-cyo, Toyohashi 441, Japan

2. Behavior of Liquid Sheet in Cocurrent Gas Stream

The representative visual wave on the liquid sheet in a cocurrent gas stream appears in the vicinity of the nozzle exit. Both the upper and lower interfaces of the liquid sheet periodically vibrate with the same phase. The wave propagates downstream with increasing amplitude. The wavelength of the wave is much larger than the liquid sheet thickness. This large-amplitude wave motion is most marked in the behavior of a liquid sheet in the cocurrent gas stream,^{(2),(3)} as shown in Fig. 1, where, Re is the Reynolds number defined as $Re = u_0 b_0 / \nu$, S is the dimensionless surface tension (reciprocal of the Weber number) defined as $S = \sigma / (2\rho b_0 u_0^2)$, and u_0 and b_0 are the mean liquid injection velocity and the half-thickness of the liquid sheet at the nozzle exit, respectively. (x, y, z) are the Cartesian coordinates. ν and ρ are, respectively, the kinetic viscosity and the density of liquid, and σ is the surface tension.

When the value of Re is small, a streamwise rivuletlike wave also appears near the disintegration point of the liquid sheet where the wave amplitude of the liquid sheet is largest, as shown in Fig. 1(a). The liquid sheet periodically breaks into fine droplets. On the other hand, when the value of Re is larger than about 400, as shown in Fig. 1(b), a spanwise finely

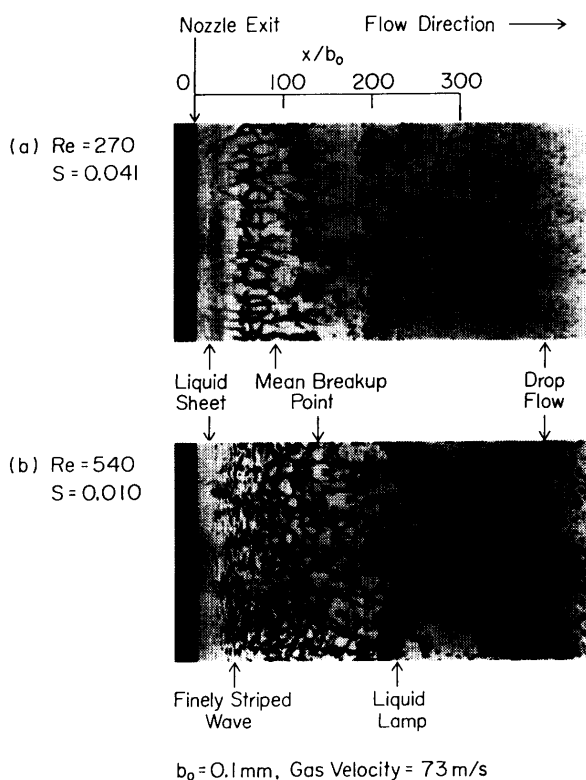


Fig. 1 Breakup patterns of liquid sheet in the gas stream

striped interfacial wave pattern appears on the smooth interface of the liquid sheet in the vicinity of the nozzle exit. The fine interfacial waves hardly affect the large-amplitude wave, but the rivuletlike wave disappears when the fine interfacial waves appear. The wavelength of the fine interfacial wave is much smaller than that of the large-amplitude wave (about 1/10). When the fine interfacial waves appear, the liquid sheet is perforated at the place where the amplitude of the fine interfacial waves becomes large, and disintegrates into not only fine but also fair-sized droplets and ligaments. That is, the fine interfacial waves greatly affect the disintegration process of the liquid sheet in the cocurrent gas stream. This wave pattern depends closely upon the value of Re , but scarcely depends on the gas-liquid relative velocity. Therefore, the fine interfacial waves seem to be mainly due to the internal disturbance of the liquid sheet rather than the aerodynamic interaction between the gas stream and the liquid sheet interface. However, the mechanism of the fine interfacial wave inception should be discussed in greater detail because the disturbance wave appears even though the liquid flow in the nozzle is laminar.

3. Behavior of Liquid Sheet in Stationary Atmosphere

Many studies on liquid sheet disintegration in the cocurrent gas stream have been reported. However, most of them focus on the large-amplitude liquid sheet wave, and the fine interfacial waves have not yet been described sufficiently. Because the fine interfacial waves were more clearly observed on the liquid sheet in a stationary atmosphere than in a cocurrent gas

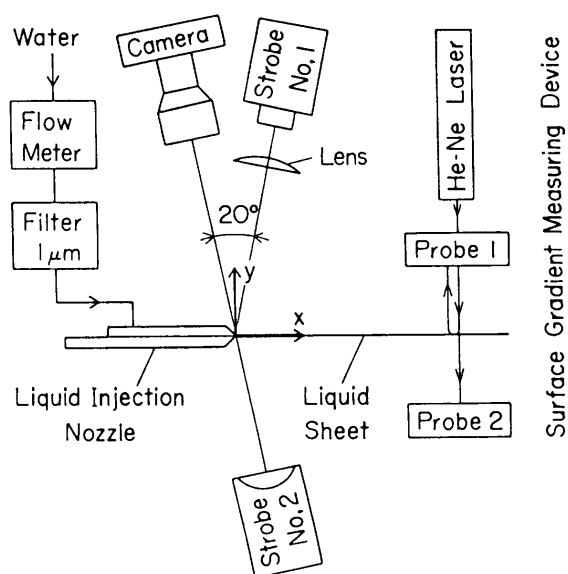


Fig. 2 Experimental apparatus

stream, the flow pattern of the liquid sheet in a stationary atmosphere was investigated experimentally to clarify the inception mechanism of the fine interfacial waves.

3.1 Experimental apparatus

Figure 2 shows a schematic diagram of the experimental apparatus. Tap water, as the liquid medium, is filtered to remove dirt particles larger than $1\ \mu\text{m}$, and is injected from the nozzle into stationary air. The nozzle has a plane thin (from 0.2 mm to 1.0 mm) rectangular duct. The spanwise width of the duct is 100 mm, and the length of the duct is 100 mm. The duct wall is smooth. The nozzle span is arranged in the direction of gravity.

The liquid sheet thickness, measured using contact needles, was confirmed to be uniform in the spanwise direction of the nozzle. The two-dimensional liquid flow field was formed approximately except at the edges of the liquid sheet ($z = \pm 50\ \text{mm}$). The narrow liquid flow in the nozzle was confirmed to be laminar from the results of measuring pressure drop along the nozzle duct when the value of Re was smaller than about 700.

The interfacial wave pattern of the liquid sheet was observed using either strobe-1 (the reflected light from the interface) or strobe-2 (the transmitted light through the liquid sheet). The configuration and the growth process of the fine interfacial waves were also observed by the surface gradient measuring device.⁽⁵⁾

3.2 Experimental results and discussion

Figure 3 shows the instantaneous photographs of the liquid sheet in the stationary atmosphere taken by strobe-1. They present the representative wave patterns. The large-amplitude liquid sheet wave, which is marked in the cocurrent gas stream, hardly appears in the stationary atmosphere. However, the finely striped interfacial wave pattern is more clearly observed. The interfacial wave pattern of the liquid sheet depends closely upon the liquid injection velocity from the nozzle (the value of Re), and can be classified into the following five representative patterns.

(a) Smooth flow (abbreviated as "Smooth" in figures): When Re is relatively small, the interface of the liquid sheet is smooth and flat like a mirror surface, as shown in Fig. 3(a).

(b) Two-dimensional wave flow (TD-Wave): When Re becomes large, the roughly two-dimensional and finely striped waves begin to appear on the smooth interface in the vicinity of the nozzle exit, as shown in Fig. 3(b). The phase velocity of these waves is of the same order as the liquid injection velocity. The wavelength of these waves scarcely varies with the downstream position and the liquid injection velocity. The dimensionless wave number ab_0 is about 0.8.

These waves can be clearly recognized by reflected light, but are hardly recognized by transmitted light. This means that the amplitude of the two-dimensional wave is very small compared with the liquid sheet thickness.

(c) Evolved two-dimensional wave flow (TD'-Wave): When Re becomes larger, the two-dimensional wave grows, and a more obvious striped pattern can be partially observed, as shown in Fig. 3(c). This partially evolved wave can be clearly recognized by transmitted light. It deforms and looks like a dimple in the downstream area.

(d) Pebble wave flow (P-Wave): When Re becomes larger than the value in Fig. 3(c), the partially evolved waves grow further, and the spots like dimples with the finely striped pattern are formed, as shown in Fig. 3(e). The interface becomes rough and presents a pebbly pattern at position far from the nozzle exit.

(e) Sandpaperlike wave flow (S-Wave): When Re becomes larger, the interface of the liquid sheet in

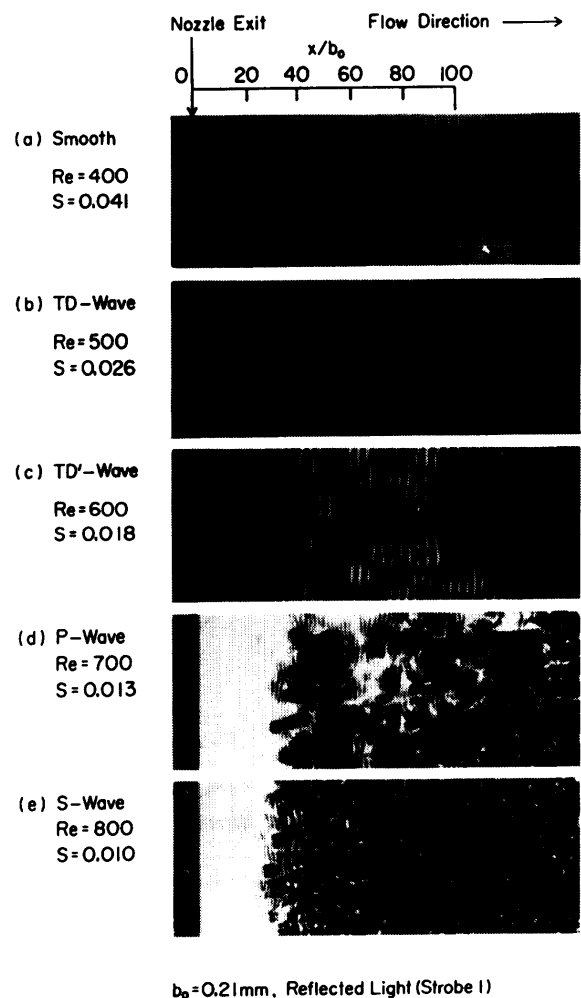


Fig. 3 Interfacial pattern of liquid sheet in stationary atmosphere

the downstream area is quite rough, although the evolved two-dimensional wave and the pebble wave are still recognized near the nozzle exit. The liquid sheet jet transits to the turbulent flow through the entire downstream area of the liquid sheet. It is seen from the photographs taken through transmitted light that this wave is formed by a combination of many pebbles.

Figure 4 shows the flow regime diagram for Re and S , at which the above five patterns are observed in $50 \leq x/b_0 \leq 150$. It is seen from this figure that the critical value of Re for the inception of the two-dimensional wave is roughly constant (about 450) in this experiment. On the other hand, the critical value of Re from the two-dimensional wave to the evolved two-dimensional wave and the critical value of Re from the evolved two-dimensional wave to the pebble wave increase with the increase of S . These results suggest that the surface tension has little effect on the inception of the interfacial wave, but suppresses the transition of interfacial wave. If the liquid sheet is relatively thick and the value of S is relatively large, the evolved two-dimensional wave in the vicinity of the nozzle exit transits directly to the sandpaperlike wave, that is, to the turbulent flow, without the transition to the pebble wave.

As mentioned above, with the increase of liquid injection velocity, the small disturbance in the liquid sheet grows, and then the two-dimensional wave appears on the interface. The two-dimensional wave evolved to deform in a three-dimensional fashion and the disturbance spots are formed. Finally, the interface of the liquid sheet is covered with numerous spots, and the liquid sheet jet transits to turbulent flow. The pattern of this disturbance spot is similar to that of the plane boundary layer⁽⁶⁾. The transition process of the interfacial wave is similar to that of liquid film flow on a plane plate⁽⁷⁾ and of a radial free

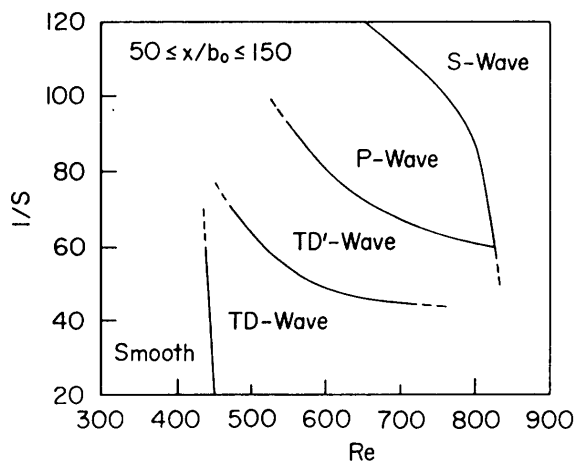


Fig. 4 Flow regime diagram

liquid sheet jet⁽⁸⁾. The flow mechanism of the liquid sheet jet may also be similar to that of these flows.

The gradients of both liquid sheet interfaces were measured simultaneously using the surface gradient measuring device⁽⁵⁾ to clarify the configuration of the interfacial wave. Figure 5 shows (I) the time series of the gradient, ζ_1 , ζ_2 , of both interfaces of the liquid sheet and (II) their cross correlation. It is seen from the figure that both interfaces periodically vibrate with almost the same phase and amplitude in the vicinity of the nozzle exit. The small fluctuation grows to become the interfacial wave in the downstream area. This short-period fluctuation is striking, and a long-period beat (about 0.7 ms) is also shown in Fig. 5.

Figure 6 shows the variation of the root mean square of the gradient, $\sqrt{\zeta_1^2}$, which is approximately proportional to the amplitude of the interfacial wave. It can be seen from this figure that the larger the value

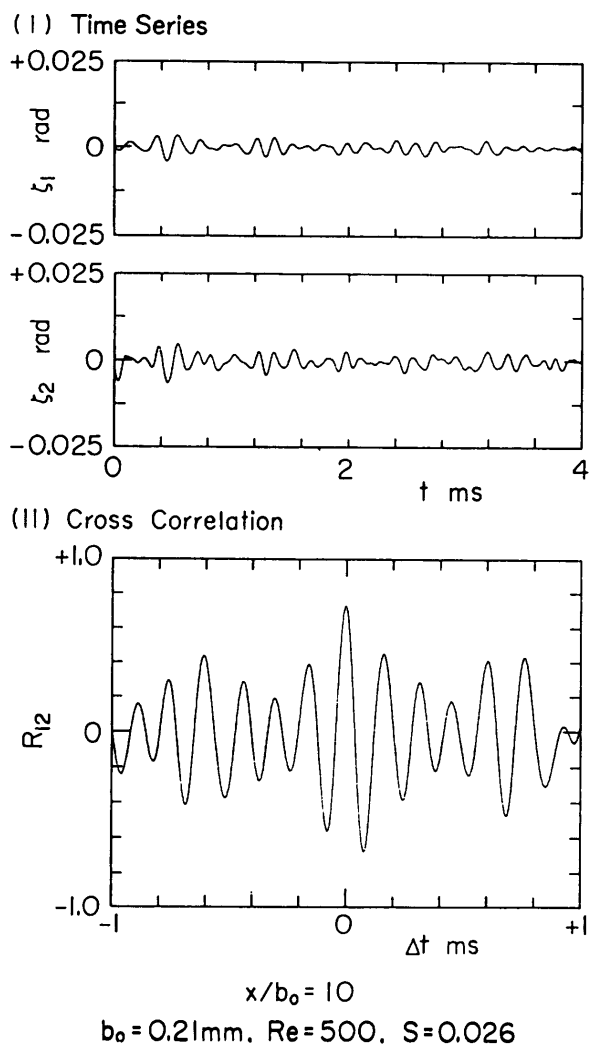


Fig. 5 Interfacial gradient

of Re , the larger the amplitude of the interfacial wave. There exist two peaks on every curve in Fig. 6. The spectral distribution of the interfacial gradient spreads widely downstream of the first peak location, and there exist many spectral peaks downstream of the second peak location, the growth and the evolution of the interfacial wave also seem to relate to the nonlinear wave interaction (not shown).

4. Instability Analysis of Liquid Sheet

It was shown in the previous chapter that the fine interfacial wave pattern is due to the internal disturbance within the liquid sheet flow. However, the mechanism has not been sufficiently clarified because of difficulties with measurement. Therefore, it is important to numerically analyze the internal instability within the liquid sheet flow.

4.1 Theoretical model

The radial free liquid sheet jet⁽⁸⁾ and the liquid film flow on a plane plate⁽⁹⁾ with the antisymmetrical velocity profile have been numerically analyzed by the linear internal stability theory. However, the free surface flow with the symmetrical velocity profile has not yet been analyzed. Hence, the instability of the free liquid sheet with the symmetrical velocity profile was analyzed based on the internal instability theory. The contact needle measurement revealed that the variation of liquid sheet thickness along the downstream distance was relatively small. Another experiment also revealed that the wave pattern during the inception stage of the interfacial wave was almost two-dimensional and was scarcely affected by the

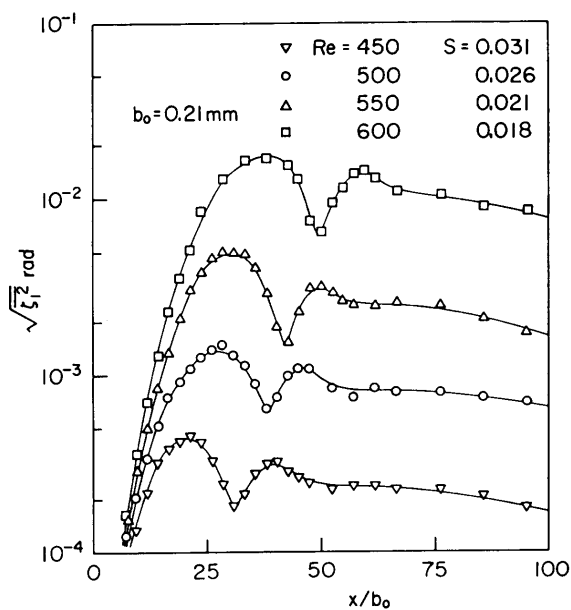


Fig. 6 Variation of root mean square of interfacial gradient with distance downstream from nozzle exit

surrounding gas flow condition, and the wave amplitude was very small compared with the liquid sheet thickness. Under the consideration of these results, and ignoring the effect of aerodynamic interaction, the instability of the two-dimensional and parallel liquid sheet was analyzed numerically.

According to the conventional method, the Orr-Sommerfeld equation which dominates the amplitude function ϕ of disturbance and the boundary condition equations on the interfaces were given as follows;

$$iaRe_s\{(u-c)(\phi^{(2)}-\alpha^2\phi)-u^{(2)}\phi\} = \phi^{(4)}-2\alpha^2\phi^{(2)}+\alpha^4\phi \quad (1)$$

$$i\phi^{(3)}-\{3\alpha^2i+aRe_s(u-c)\}\phi^{(1)} \pm 2S_sRe_s\alpha^3\phi/(c-u)=0 \quad (2)$$

(at $y = \pm 1$)

$$\phi^{(2)}+\{\alpha^2+u^{(2)}/(c-u)\}\phi=0 \quad (3)$$

(at $y = \pm 1$).

The above equations are nondimensionalized by the local value of the liquid sheet half-thickness b and the local value of interfacial velocity $u(b)$. $\phi^{(n)}$ is the n -th differential of ϕ with respect to y . c is the complex velocity of disturbance defined as $c = c_r + ic_i$, where c_r is the velocity and c_i is the growth rate. α is the wave number of disturbance. Dimensionless parameters Re_s and S_s are defined as $Re_s = bu(b)/\nu$ and $S_s = \sigma/\{2\rho bu(b)^2\}$, respectively.

Based on the experimental results, the sinuous (sinusoidal) disturbance in which both interfaces vibrated in the same phase, and the dilational disturbance in which the two interfaces vibrated in opposite phases were chosen as the subject of this analysis. The following boundary conditions on the centerline were introduced.

$$\phi^{(1)}=0 \quad (\text{at } y=0, \text{ for sinuous disturbance}) \quad (4)$$

$$\phi^{(2)}=\phi=0 \quad (\text{at } y=0, \text{ for dilational disturbance}) \quad (5)$$

The laminar solution on the liquid sheet thickness and the velocity profile in the liquid sheet were determined by Lienhard's method⁽¹⁰⁾. The eigenvalue problem of Eq.(1) to Eq.(4) or Eq.(1) to Eq.(3) and Eq.(5) over the range of $0 \leq y \leq 1$ was solved numerically by Thomas's method⁽¹¹⁾. The results were rearranged into the ordinary form based on b_0 and u_0 .

4.2 Numerical results and discussions

The instability of the plane liquid sheet was first analyzed numerically in the case of negligibly small surface tension. Because the velocity profile curve has the inflection points, the liquid sheet becomes unstable (the value of the growth rate is positive) at any downstream distance. Figure 7 shows an example of the numerical results on the liquid sheet instability for the sinuous disturbance. This figure shows the relationship of the growth rate, c_i/u_0 , to the downstream distance, $x/(Reb_0)$, from the nozzle exit and the wave

number, ab_0 . The growth rate for a certain wave number decreases with the increase of the downstream distance. In the region bounded by the two dash-dotted lines in the figure, the constant growth rate curve (solid line) has the maximum for the downstream distance at a certain wave number. This means that there exists maximum growth rate for that wave number. However, outside of the two dash-dotted lines, the downstream distance for constant growth rate decreases with the increase in wave number. That is, there are two kinds of instability modes. The characteristics of each instability mode seem to be similar to those of the hard-mode instability and the soft-mode instability of liquid film flow on a plane plate⁽⁹⁾, respectively.

It is also confirmed numerically that the above characteristics of instability for the sinuous distur-

bance are similar to those for the dilational disturbance. However, the wave number range and the growth rate of the hard-mode instability for the dilational disturbance differ from those for the sinuous disturbance (not shown).

Figure 8 shows the comparison between the experimental results and the numerical results. In this figure, all lines indicate the numerical results on the hard-mode instability. The solid lines show the variation of the wave number for the downstream distance, at which growth rate has a maximum. The dash-dotted lines and the broken lines show the maxima of growth rate and the wave velocities for these wave numbers, respectively. Because the hard-mode is limited within a narrow range of wave number at the downstream region (see Fig. 7), the maximum growth rate does not exist at the downstream region shown by the solid circle symbol; then the soft-mode dominates. These numerical results support the experimental result that the two-dimensional wave was damped in the region far from the nozzle exit. The maximum growth rate for the sinuous disturbance is always larger than that for the dilational disturbance. This result also supports the experimental results that both interfaces of the liquid sheet periodically vibrate in the same phase. Furthermore, the value of the wave number at which the numerical growth rate for sinuous disturbance is a maximum agrees approximately with the wave number of the interfacial wave obtained in the experiment (c.f. open symbols in the figure). These agreements between the numerical results and the experimental results support the validity of this analytical model. That is, the inception of interfacial waves on the liquid sheet depends on the hard-mode instability for the sinuous disturbance.

Figure 9 shows the effect of Reynolds number Re on the hard-mode instability for the sinuous disturbance. It is seen from the figure that the maximum of the growth rate (dash-dotted line) decreases with the

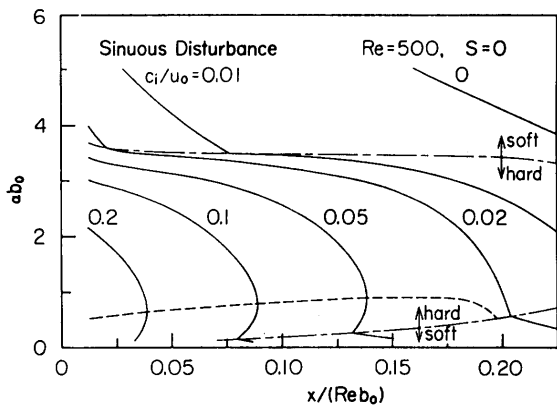


Fig. 7 Instability curves for sinuous disturbance

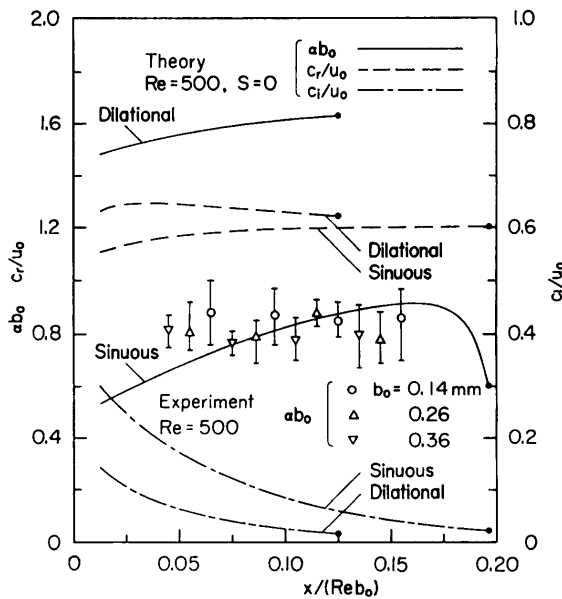


Fig. 8 Comparison of experimental results with numerical results on hard-mode instability

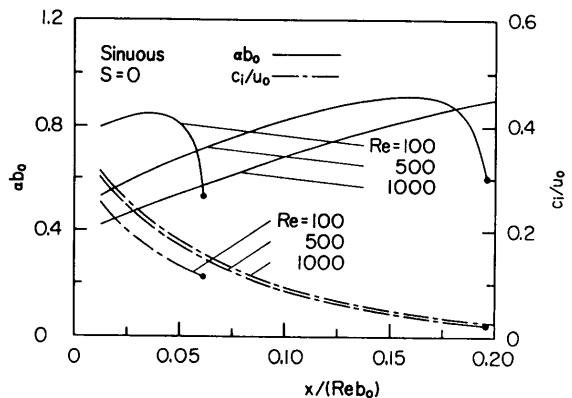


Fig. 9 Effect of Re on hard-mode instability

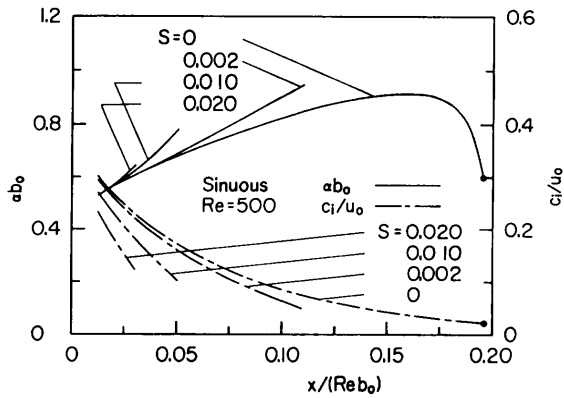


Fig. 10 Effect of S on hard-mode instability

decrease of Re , but the maximum of the growth rate is always positive. Many kinds of actual disturbances can be supposed as the initial disturbance of the instability wave. The earlier study⁽¹²⁾ on the plane Poiseuille flow suggested that there were weak disturbances even at a small value of Re , although the liquid flow could be estimated to be laminar within $Re < 700$. Furthermore, the wave number of the two-dimensional wave on the free liquid sheet is of the same order as the wave number of the two-dimensional disturbance around the turbulent spot in the plane Poiseuille flow⁽¹³⁾. These discussions suggest that the initial disturbance of the interfacial wave on the liquid sheet is due to weak disturbances in the nozzle.

Figure 10 shows the effect of the dimensionless surface tension S on the hard-mode instability for the sinuous disturbance. As can be seen from the figure, the growth rate decreases and the wave number increases with the increase of S . That is, the liquid sheet flow tends to be stabilized by the surface tension. This tendency corresponds to the experimental result that the transition values of Re increase with the increase of S . It can be seen from these results that the effects of internal instability on the atomization process may be more serious in the case of the low-surface-tension liquid, such as gasoline or alcohol.

Since the above numerical results were based on the linear theory, it was not sufficient to explain the grown interfacial wave with large amplitude. However, the quantitative relationship between the interfacial wave and the liquid sheet flow condition was described in detail. The relation of the Reynolds number and the dimensionless surface tension to the liquid sheet disintegration caused by the interfacial wave were clarified.

5. Conclusions

The fine interfacial wave pattern on the free thin

liquid sheet was investigated experimentally and numerically. The results were summarized as follows.

(1) The fine interfacial wave on the thin liquid sheet in a cocurrent gas stream greatly affected the disintegration process of the liquid sheet.

(2) The interfacial wave patterns on the liquid sheet in a stationary atmosphere could be classified into five representative patterns. The ranges of these patterns were determined by the dimensionless values of Re and S .

(3) It was found that the configuration of fine interfacial waves on the liquid sheet in a stationary atmosphere was the periodic vibration of both liquid sheet interfaces with the same phase and amplitude.

(4) It was found numerically that the plane liquid sheet was unstable for both the sinuous disturbance and the dilational disturbance, and that the basic wave characteristics of the interfacial wave could be approximately estimated by the numerical results.

(5) Comparing the numerical results and the experimental results, it was shown that the interfacial wave was closely related to the internal disturbance which resulted due to the internal instability of the liquid sheet, and that the inception of the interfacial wave corresponded to the hard-mode instability for the sinuous disturbance.

References

- (1) Lefebver, A. H., *Prog. Energy Combust. Sci.*, 6 (1980), p. 233.
- (2) Arai, T. and H. Hashimoto, *Trans. JSME (in Japanese)*, 51-470B(1985), p. 3336.
- (3) Arai, T. and Hashimoto, H., *Bull. JSME*, 28 (1985), p. 2652.
- (4) Suzuki, T. and Hashimoto, H., *Proceedings of 9th International Symposium on Jet Cutting Technology*, (1988), p. 165.
- (5) Suzuki, T. and Hashimoto, H., *Japanese J. Multi-phase Flow (in Japanese)*, 4-3(1990), p. 210.
- (6) Frost, W. and Moulden, T. H., *Handbook of Turbulence*, Vol. 1, (1977), Plenum Press.
- (7) Fukano, T., Ito, A., Miyabe, K. and Takamatsu, Y., *Trans. JSME (in Japanese)*, 45-390(1979), p. 172.
- (8) Azuma, T., *Proceedings of 4th International Conference on Liquid Atomization and Spray Systems*, (1988), p. 185.
- (9) DeBruin, G. J., *J. Eng. Math.*, 8(1974), p. 259.
- (10) Lienhard, J. H., *J. Basic. Eng.*, 90-2(1968), p. 262.
- (11) Thomas, L. H., *Phys. Review*, 91-4(1953), p. 780.
- (12) Mizunuma, H. and Kato, H., *Trans. JSME (in Japanese)*, 53-488, B(1987), p. 1214.
- (13) Henningson, D. S. and Alfredsson, P. H., *J. Fluid Mech.*, 178(1987), p. 405.